Morales Maqueda MA, Penna NT, Williams SDP, Foden PR, Martin I, Pugh J.
Water surface height determination with a GPS Wave Glider: A demonstration in Loch Ness, Scotland.
***Journal of Atmospheric and Oceanic Technology* 2016, 33(6), 1159-1168.**

Water Surface Height Determination with a GPS Wave Glider: A Demonstration in Loch Ness, Scotland

M. A. MORALES MAQUEDA

School of Marine Science and Technology, Newcastle University, Newcastle upon Tyne, United Kingdom

N. T. PENNA

School of Civil Engineering and Geosciences, Newcastle University, Newcastle upon Tyne, United Kingdom

S. D. P. WILLIAMS AND P. R. FODEN

National Oceanography Centre, Natural Environment Research Council, Liverpool, United Kingdom

I. MARTIN

School of Civil Engineering and Geosciences, Newcastle University, Newcastle upon Tyne, United Kingdom

J. PUGH

National Oceanography Centre, Natural Environment Research Council, Liverpool, United Kingdom

(Manuscript received 12 August 2015, in final form 5 November 2015)

ABSTRACT

A geodetic GPS receiver has been installed on a Wave Glider, an unmanned water surface vehicle. Using kinematic precise point positioning (PPP) GPS, which operates globally without directly requiring reference stations, surface heights are measured with ~0.05-m precision. The GPS Wave Glider was tested in Loch Ness, Scotland, by measuring the gradient of the loch's surface height. The experiment took place under mild weather, with virtually no wind setup along the loch and a wave field made mostly of ripples and wavelets. Under these conditions, the loch's surface height gradient should be approximately equal to the geoid slope. The PPP surface height gradient and that of the Earth Gravitational Model 2008 geoid heights do indeed agree on average along the loch (0.03 m km^{-1}). Also detected are 1) ~0.05-m-sized height changes due to daily water pumping for hydroelectricity generation and 2) high-frequency (0.25–0.5 Hz) oscillations caused by surface waves. The PPP heights compare favorably (~0.02-m standard deviation) with relative carrier phase–based GPS processing. This suggests that GPS Wave Gliders have the potential to autonomously determine centimeter-precise water surface heights globally for lake modeling, and also for applications such as ocean modeling and geoid/mean dynamic topography determination, at least for benign surface states such as those encountered during the reported experiment.

1. Introduction

Accurate water surface height measurements are needed for the investigation and modeling of the marine geoid, the mean dynamic topography (MDT) of the ocean, and the dynamics of shelf and coastal environments. Sea level measurements rely predominantly on the use of coastal tide gauges and satellite altimetry. Tide gauge data have fine temporal resolution (minutes to hours) and are the most reliable source of long-term sea level change, but their spatial representativeness is limited to the area surrounding the tide gauge. Extrapolating sea levels from tide gauge data is problematic, even when correcting for land movement and

Denotes Open Access content.

Corresponding author address: M. A. Morales Maqueda, School of Marine Science and Technology, Newcastle University, Armstrong Building, Newcastle upon Tyne NE1 7RU, United Kingdom.
E-mail: miguel.morales-maqueda@ncl.ac.uk

DOI: 10.1175/JTECH-D-15-0162.1

averaging sea level records over many tide gauge stations (Jevrejeva et al. 2006). The interannual variability of tide gauge–based sea level, for example, is perhaps several times larger than sea level variability over the open ocean derived from altimetry (Prandi et al. 2009). Theory also suggests that tide gauges do not reflect the dynamics of sea level near and beyond the continental shelf break (Huthnance 2004). In contrast, altimetry data have nearly global coverage, but their spatial (10–100 km) and temporal (10–30 days) resolutions are relatively coarse. In addition, since the corrections applied to the altimetric waveforms are better suited for the open ocean than for the coast, distortions of the waveforms within ~10 km of the coast need to be corrected (Gommenginger et al. 2011).

GPS devices are an ideal complement to tide gauges and altimetry, especially in bridging the above-mentioned gaps in temporal and spatial resolutions left by the latter two systems and in improving the quality of measurements near coastal areas. GPS can provide geocentric measurements of instantaneous sea level with a precision of 0.05–0.10 m (e.g., Kuo et al. 2012)—hence, similar to the altimetry precision of ~0.03 m (Palanisamy et al. 2015), but with the temporal resolution of tide gauges, and may be deployed anywhere in the ocean. GPS devices have been deployed on buoys for altimetry calibration (e.g., Watson et al. 2003), mean sea surface and geoid determination (e.g., Bonnefond et al. 2003; Rocken et al. 2005), definition of data of offshore moorings and structures (Watson et al. 2008), wave measurement (e.g., Cardellach et al. 2000), and river level heighting (Moore et al. 2000). However, as with tide gauges, they only provide measurements at discrete point locations. GPS devices on board commercial ships have been used to measure sea surface topography (Foster et al. 2009) and for tsunami detection (Foster et al. 2012), but they have the drawbacks of requiring onboard radar altimetry to correct for variations in the ship's free board and being constrained to shipping routes.

A remedy to the limitations of GPS buoy- and ship-based measurements is the installation of GPS devices on unmanned surface vehicles (USVs) capable of both keeping station, thus acting as buoys, and engaging in survey missions over user-controlled routes. We report on results of the first test of such an integrated GPS–USV system for centimeter-precise water surface height determination, comprising a geodetic Trimble GPS NetR5 receiver and a Trimble Zephyr 2 antenna mounted on a Liquid Robotics Wave Glider SV2 (GPS Wave Glider). The Wave Glider is a surfboard-sized unmanned vehicle that converts wave energy into forward propulsion, without the need of fuel or electric power. It is a proven technology that has been successfully deployed on many missions (e.g., Willcox et al. 2009; Daniel et al. 2011).

As a demonstration of the GPS Wave Glider concept, we deployed the instrument in Loch Ness, Scotland, which provided an easily accessible and controlled, safe environment for our trial. Winds were weak for the duration of the experiment, resulting in low-amplitude waves (less than 0.1–0.2 m) at the loch's surface. Hence, surface conditions were comparable to those that would be experienced for sea states between 0 and 3 if the Wave Glider were deployed in the open ocean. Such sea states are fairly common during the summer months, for example, in the western North Sea, they occur more than 40% of the time between May and August (Fugro GEOS 2001). In the absence of winds or other dynamical forcing (maximum wind setup on the loch's northern end during the experiment is calculated as below 1 mm), the water surface should lie on a gravity equipotential and, the water level of Loch Ness being only about 16 m above Ordnance Datum Newlyn (ODN), was expected to be approximately parallel to the geoid. The slope of the loch's surface will therefore be compared in this paper with the geoid gradient from the Earth Gravitational Model 2008 (EGM2008; Pavlis et al. 2012, 2013), which is $-0.03\ \mathrm{m\ km^{-1}}$ from the south to the north ends of the loch. In addition, Loch Ness undergoes a daily surface height change that had a range of around 0.05 m during the period of our measurements, and is caused by pumping of water from Loch Ness to Loch Mhor, water which is later released back to Loch Ness for the generation of hydroelectric power at Foyers (Fig. 1). The aim of this study is to assess the GPS Wave Glider's ability to measure the spatial and temporal variations in Loch Ness surface height arising from the geoid gradient and the daily pumping of water, and also to consider the presence and nature of observed high-frequency GPS height variations due to the wave field. This serves as a demonstration of the GPS Wave Glider's measurement precision and potential for applications such as the determination and modeling of the marine geoid and the ocean's MDT, both of which require centimeter-precise measurements of water surface heights.

2. Equipment, deployment, and data acquisition

For the Loch Ness deployment, besides integrating the Trimble NetR5 geodetic GPS receiver and Zephyr 2 antenna, the GPS Wave Glider included an Airmar CS4500 ultrasonic water speed sensor (nominal accuracy of $0.05\ \mathrm{m\ s^{-1}}$), a SignalQuest SQ-SI-360DA solid-state microelectromechanical system (MEMS) inclinometer (stated accuracy and smallest recorded measurement unit of ±1° and 0.1°, respectively), an echo sounder, a downward-looking acoustic Doppler current profiler,

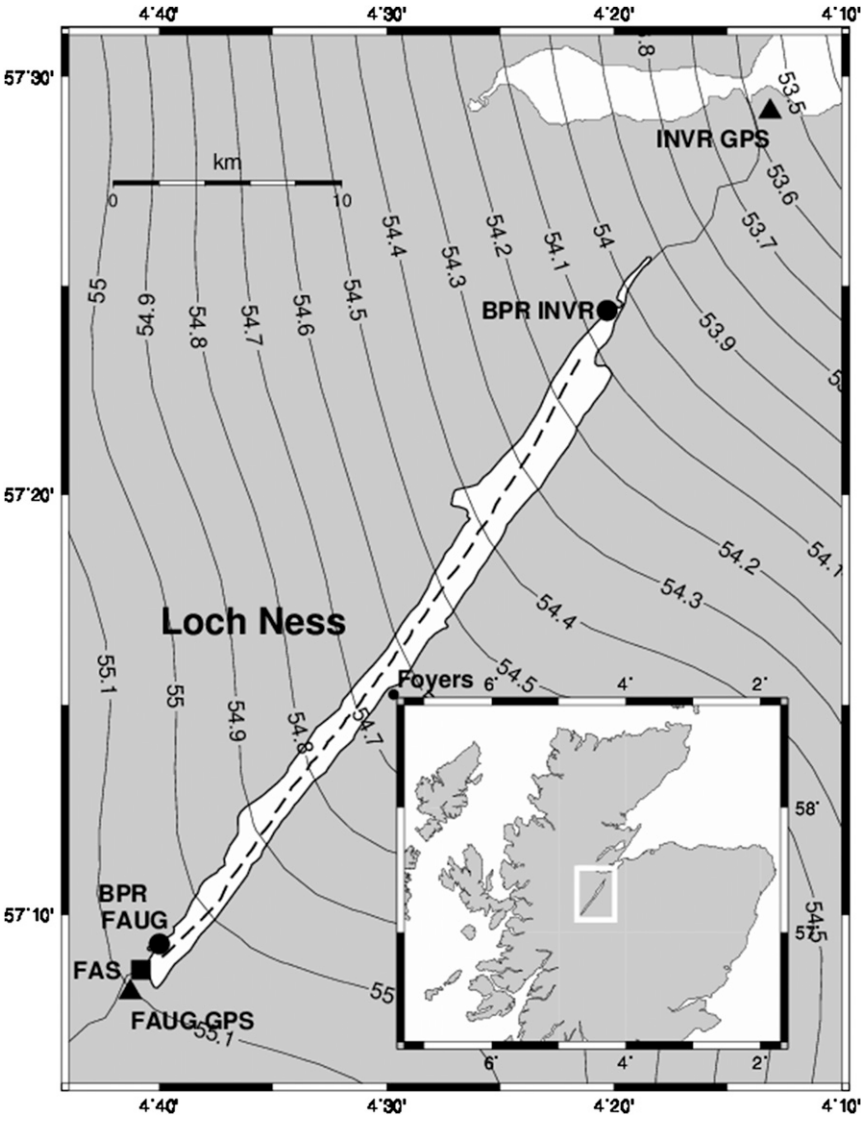

FIG. 1. (inset) Highlands of Scotland, showing the location of Loch Ness (inside the white-edged rectangle). (larger frame) A zoom over Loch Ness. Water-covered areas are shown in white and land in gray. The track of the Wave Glider is superimposed as a dashed line. Also shown are the positions of BPR FAUG and BPR INVR, FAS tide gauge, FAUG GPS) and INVR GPS, and the location of the hydroelectric power station at Foyers. The location of the barometer is indistinguishable from that of BPR FAUG in the map. The contour lines correspond to EGM2008 geoid heights (m).

and a PAMBuoy passive acoustic monitoring device. The setup is shown in Fig. 2. To ensure unobstructed Zephyr 2 GPS antenna-to-satellite visibility, the manufacturer-provided Airmar PB200 meteorological mast, Automatic Identification System (AIS) antenna, and active radar reflector were removed.

To measure the geoid gradient along the loch, the GPS Wave Glider was deployed from 57°08′51″N, 004°40′03″W, near Fort Augustus at the southwest end of the loch, and fully autonomously navigated to 57°23′13″N, 004°21′31″W, near Inverness at the northeast end of the loch, along a central trajectory as shown in Fig. 1. The survey started at 1136 UTC 14 March 2013 and finished at 1259 UTC 15 March 2013, with the GPS Wave Glider covering a distance of about 32 km in approximately 25 h. Dual-frequency carrier phase and code GPS data from the Trimble NetR5, together with inclinometer data, were collected at 1 Hz throughout, with the water speed sensor data and navigation information necessary for piloting the Wave Glider telemetered via Iridium every 5 min during

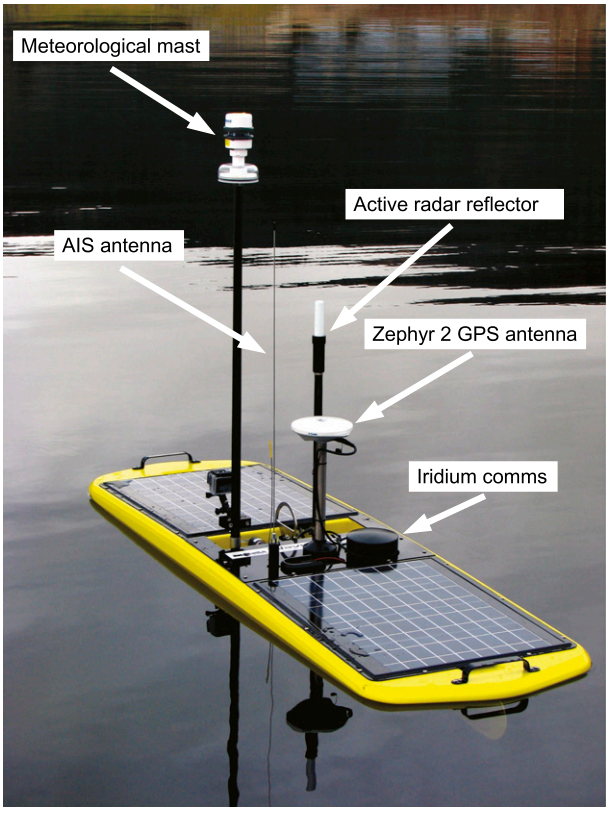

FIG. 2. Wave Glider in Loch Ness during trials preceding the loch transect. For the glider's deployment along the loch transect, the meteorological mast, active radar reflector, and AIS antenna were abated so as not to obstruct the GPS satellite visibility from the Zephyr 2 antenna.

the first 4 h of the survey and every 15 min thereafter. The sole perturbation of the glider during the survey took place between 1717:30 and 1722:30 UTC 14 March 2013, when the vehicle was inspected at close range by us from a boat, resulting in severe masking of the GPS antenna-to-satellite line of sights during this time.

To provide control measurements of variations in relative water level, a Paroscientific Digiquartz barometer model 765-15A pressure standard, with the manufacturer's accuracy of 0.0008 dbar, and two Richard Branker Research TGR-1050P bottom pressure recorders (BPRs), with the manufacturer's accuracy and resolution of 0.01 and 0.0002 dbar, respectively, were deployed for the duration of the survey. The barometer was installed at the Old Pier House (57°09′07″N, 004°40′18″W), very close to the location indicated as BPR Fort Augustus (FAUG) in Fig. 1, and was set to record surface air pressure at 0.2 Hz. The BPRs were deployed at 57°09′18″N, 004°40′00″W (BPR FAUG) and 57°24′24″N, 004°20′18″W [(BPR Inverness (INVR)] and recorded at 1 Hz. We also obtained 15-min data from the Scottish Environment Protection Agency (SEPA) tide gauge at Fort Augustus (FAS).

Since the meteorological mast on the Wave Glider had been uninstalled for this deployment, we do not have information on the wind speed and direction during the vehicle's passage. The barometer shows a nearly linear drop in surface air pressure, from 1007.5 to 991 hPa, between the deployment time and 0430 UTC 15 March 2013. The pressure then remained at 990–992 hPa until the end of the experiment. Wind data from the Met Office Integrated Data Archive System (MIDAS) stations 67 and 105, located in the vicinity of Loch Ness, indicate a persistent southerly-southwesterly—that is, ~0° to ~45° relative to the loch's long axis—light or gentle breeze of about 3–5 $m\,s^{-1}$ throughout the deployment. This is consistent with the wave field in the loch comprising mostly wavelets. Accordingly, the glider's hourly averaged speed was only 0.35 $m\,s^{-1}$ ($\sigma = 0.08\,m\,s^{-1}$).

3. GPS data processing

The GPS data collected by the Trimble NetR5 were postprocessed to estimate positions every 1 s using the kinematic precise point positioning (PPP) mode, as would be needed in the open ocean, where no reference station data would be normally available, but also in relative kinematic mode for quality control with respect to Ordnance Survey GPS reference stations at Fort Augustus and Inverness (FAUG GPS and INVR GPS, respectively, in Fig. 1), both Leica GS10 receivers logging at 1 Hz. The glider was never farther than about 20 km from one of these reference stations during the survey. The NASA JPL Global Navigation Satellite System (GNSS)-Inferred Positioning System (GIPSY) V6.2 software was used for the kinematic PPP GPS processing, fixing reprocessed JPL "repro1 (reprocessing campaign 1)" satellite orbits and 30-s clocks, applying ECMWF a priori zenith hydrostatic delays (Boehm et al. 2006b), and the zenith wet delay (process noise of $2.0 \times 10^{-8}\,km\,s^{-1/2}$ and gradients estimated, using the Vienna Mapping Function 1 (VMF1) gridded mapping function (Boehm et al. 2006b). A coordinate process noise of $1.0 \times 10^{-3}\,km\,s^{-1/2}$ was used, together with elevation angle–dependent observational weighting, a 10° elevation angle cutoff, and float ambiguities. International GNSS Service reference frame 2008 (IGS08) absolute antenna phase center models were applied, with solid Earth tides modeled according to International Earth Rotation and Reference Systems Service (IERS) 2010 conventions (Petit and Luzum 2010). The reference stations FAUG and INVR were similarly coordinated using GIPSY (but in static mode), using the same time span of data. These coordinates were then held fixed in the

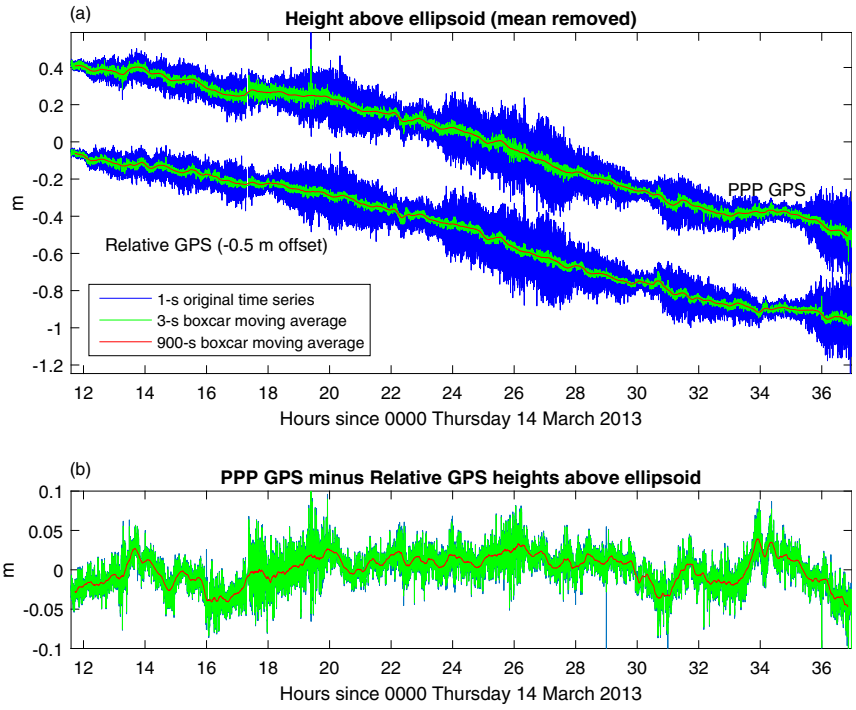

FIG. 3. (a) Time series of heights above the ellipsoid of the GPS antenna reference point calculated during the Loch Ness passage. The top blue curve corresponds to the kinematic postprocessed PPP GPS 1-s ellipsoidal heights (referenced to their mean value over the ~25 h of the survey, which is 70.00 m). The bottom blue curve represents the ellipsoidal heights derived from relative GPS postprocessed with respect to FAUG and INVR (also referenced to its mean value over the ~25 h of the survey, namely, 70.00 m) and offset by −0.5 m for clarity. The green and red curves are obtained by performing 3-s and 900-s boxcar moving averages, respectively, on the blue curves. (b) Difference between the PPP and relative GPS curves shown in (a).

relative GPS processing, for which the GPS Analysis at Massachusetts Institute of Technology (GAMIT) Track V1.28 software was used, computing the glider's position using a network solution. IGS08 absolute antenna phase center models were applied, the ambiguities were fixed to integers, and the tropospheric Global Mapping Function (GMF; Boehm et al. 2006a) was used but without estimating a tropospheric parameter. The GAMIT Track default coordinate process noise of 4.5×10^{-3} km s$^{-1/2}$ was applied, together with elevation angle–dependent observational weighting. Data from 1717:30 to 1722:30 UTC were excluded from the processing due to the severe signal masking described above.

4. Measured water surface height of Loch Ness

Figure 3a shows the time series of heights above the World Geodetic System 1984 (WGS84) ellipsoid of the GPS Wave Glider's Zephyr 2 antenna reference point, which we estimate was about 0.36 m above the glider's deck, which, in turn, rose above the water surface by around 0.04 m in calm water. The top curve is obtained using the kinematic PPP GPS technique. The blue curve corresponds to the 1-s time series. The clear negative trend in ellipsoidal height is mostly, as we will argue below, due to the geoid gradient along the loch. Once the linear component of the trend is removed, the time series has a standard deviation (σ) of ~0.06 m, which is commensurate with kinematic PPP precisions obtained with unobstructed sky visibility (e.g., Chen et al. 2013; Kuo et al. 2012). Moving averaging the data with a 3-s boxcar window (green curve) reduces σ to 0.04 m (approximately 50% of the time series variance is concentrated at frequencies higher than 0.25 Hz, which we investigate in section 4c). Further filtering the data with a 900-s boxcar window hardly affects σ, since there is only a 5% loss in signal variance in the frequency interval (1.1×10^{-3} Hz, 0.25 Hz). The bottom curve of Fig. 3a is the time series obtained using the relative GPS approach offset from the PPP curve by −0.5 m. There is a striking visual similarity between the PPP and relative GPS time series and, when linearly detrended, the correlations between them are 0.93, 0.87, and 0.91 for the 1-, 3-, and 900-s moving averaged time series, respectively,

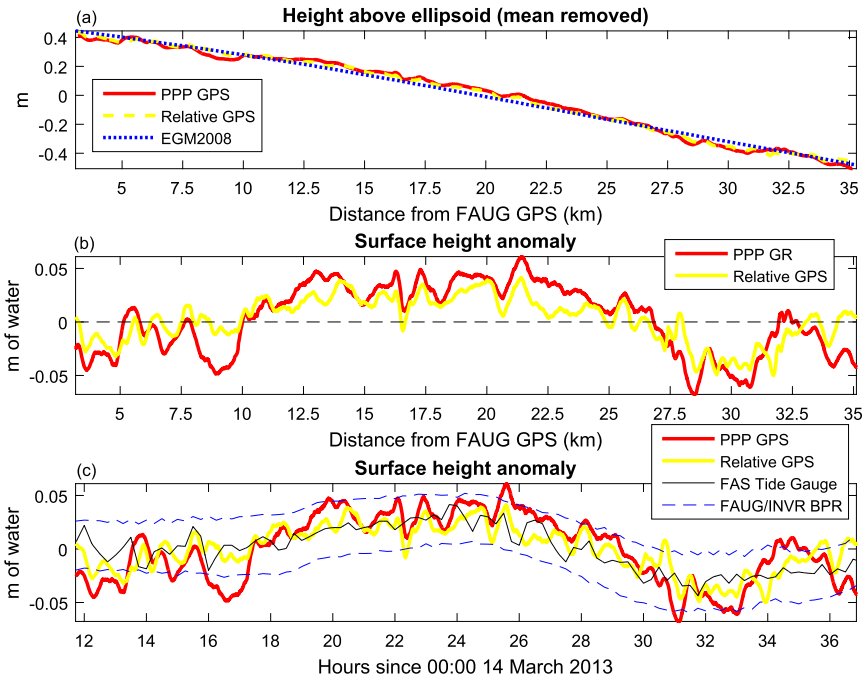

FIG. 4. (a) Kinematic PPP (red) and relative (yellow) 900-s GPS ellipsoidal heights against distance from FAUG GPS station (57°08′09.6″N, 4°41′16.8″W). Also shown are the EGM2008 (blue) geoid heights, plotted with the mean removed. (b) Surface height anomalies: Kinematic PPP GPS 900-s ellipsoidal minus EGM2008 geoid heights (red) and relative 900-s GPS ellipsoidal minus EGM2008 geoid heights (yellow) as a function of linear distance from FAUG GPS station. (c) Surface height anomalies: Kinematic PPP GPS 900-s ellipsoidal minus EGM2008 geoid heights (red) and relative 900-s GPS ellipsoidal minus EGM2008 geoid heights (yellow) as a function of time. Also shown are the 900-s time series of surface height from the FAS tide gauge (black) and the equivalent surface height derived from the FAUG BPR (offset by 0.025 m; dashed blue curve top) and INVR BPR (offset by −0.025 m; dashed blue curve bottom). The mean values have been removed from all the time series.

demonstrating the robustness of the PPP method through quality control with the relative GPS technique. The differences between the PPP and relative GPS surface height time series are shown in Fig. 3b, with a common mean of −0.005 m and standard deviations of 0.023, 0.022, and 0.017 m for the 1-, 3-, and 900-s filtered curves, respectively.

a. Comparison of GPS Wave Glider ellipsoidal heights with EGM2008 geoid heights

Since the Wave Glider speed was not uniform during the passage, the points in Fig. 3 cannot be used to interpret spatial gradients in water surface height. In Fig. 4a, the 900-s curves shown in Fig. 3a are redrawn against the horizontal distance from FAUG GPS. EGM2008 geoid heights in the tide-free system, compatible with the GPS, were computed at the 900-s latitudes and longitudes using the harmonic synthesis program (http://earth-info.nga.mil/GandG/wgs84/gravitymod/egm2008/hsynth_WGS84.f), and are also shown in Fig. 4a with both GPS and EGM2008 values plotted with their means removed. There is a very clear FAUG-to-INVR gradient in the GPS 900-s curve of $-0.03\,\mathrm{m\,km^{-1}}$, equal to that of the EGM2008 geoid heights. The agreement between the two gradients helps to validate the EGM2008 geoid model and illustrates the potential of the GPS Wave Glider for marine geoid/MDT determination. If absolute values are considered, the mean of the ellipsoidal surface height inferred from our GPS Wave Glider survey (69.65 m) is 15.25 m greater than the mean of the EGM2008 geoid heights, comparable to the stated (Pugh et al. 2011) 16-m Loch Ness elevation above mean sea level.

b. Detection of water surface height variations due to pumping

The PPP and relative GPS 900-s averaged ellipsoidal heights shown in Fig. 4a exhibit a near-cyclic variation about the EGM2008 geoid heights (Fig. 4b). To investigate if these variations can be attributed to the known daily pumping and re-release of water between Loch Ness and Loch Mhor, the PPP and relative GPS

surface height anomalies (computed by subtracting the EGM2008 geoid heights and then removing the mean) are shown in Fig. 4c against time. Also plotted are the anomalies from the FAS tide gauge and from the FAUG and INVR BPRs (after the subtraction of air pressure). The BPR and tide gauge anomalies show a clear surface height "tide" of around 0.025 m amplitude, in accordance with the known daily pumping of water. This cyclic variation in the surface height anomaly is also detected by the PPP and relative GPS 900-s time series. The excursions of the PPP GPS 900-s time series about the EGM2008 geoid heights are larger than those of the relative GPS (with standard deviations of 0.03 and 0.02 m, respectively), which we attribute to the removal of common glider and reference station satellite orbit, clock, and atmospheric errors in the relative solution but not in the PPP solution. However, the correlation between the two series is large at 0.83, which means that nearly 70% of the variance is common to the two series and that the GPS Wave Glider is able to detect low-frequency "tidal" signals of ~0.025-m amplitude. Around 50% of the variance common to the PPP and relative GPS time series is indeed accounted for by the tidal signal. If this signal is subtracted from both the PPP and relative GPS time series, the correlation of the resulting curves drops to 0.60 (i.e., just above 35% of the variance of either of the series is then explained by the other).

c. *High-frequency GPS height variations*

A final aspect of the GPS time series that we wish to explore concerns the origin and nature of the components of the signal with frequencies larger than 0.25 Hz. These frequencies contribute about half of the total variance of the surface height time series, with a potential noise source for the GPS Wave Glider being wind waves and the glider motion in response to the wave field. The periods of such motions oscillate between a small fraction of a second and a few seconds. While we have no quantitative information about surface winds and the associated wave field during the experiment, the inclinometer time series allows us to evaluate the high-frequency motions of the Wave Glider independently of the GPS data. Figure 5a shows the 1-s linearly detrended time series of Wave Glider pitch during the loch passage. There is a bias toward positive pitch that can be explained by 1) the bow of the glider tends to become elevated with respect to the stern as the vehicle moves forward and 2) the PAMBuoy mentioned in section 2 was installed astern, thus creating a weight imbalance between the stern and the bow. Figure 5b shows the 1-s time series of PPP GPS surface height anomalies: both the EGM2008 geoid heights and the FAS tide gauge elevations have been subtracted from the GPS ellipsoidal heights and a remaining linear trend of 9×10^{-4} m h^{-1} was removed. The clear visual similarity between the curves depicted in Figs. 5a and 5b is quantified in Fig. 5c, where the coherence between the inclinometer pitch and PPP GPS surface height anomalies, calculated following Welch's averaged modified periodogram method (Welch 1967), is shown. A total of 356 nonoverlapping sections were used, each 256 s long, windowed with a Hann window. The high-frequency components of both signals are very coherent, with a broad peak at a period of ~3 s (Fig. 5c), suggesting that the oscillations in PPP GPS heights with periods of up to a few seconds are largely caused by glider motions in response to surface wave activity. The amplitude of this variability appears to undergo slow modulations at time scales of a few hours, which we attribute to changes in wind forcing and hence surface wind waves. Unfortunately, there are no MIDAS stations recording wind in Loch Ness, and so we cannot relate these amplitude changes to wind changes. An analysis of surface current speed and heading, calculated from Wave Glider trajectory parameters and water speed sensor data, does not reveal any obvious current variability that could explain the observed amplitude modulation.

5. Discussion and conclusions

We have undertaken a pilot deployment of a Wave Glider SV2 equipped with a Trimble NetR5 geodetic GPS receiver, a Trimble Zephyr 2 antenna, and an inclinometer in Loch Ness, Scotland. The GPS Wave Glider traveled 32 km along the length of the loch in around 25-h, propelled by small surface wavelets. Using both PPP and relative GPS techniques, an ellipsoidal surface height gradient of -0.03 m km^{-1} was measured that matched very closely the EGM2008 geoid gradient, thus illustrating the fitness of the GPS Wave Glider for marine geoid/MDT determination. After removing the geoid gradient from the ellipsoidal GPS heights, the surface height anomalies revealed a cyclic variation of ~0.025-m amplitude that matched tide gauge and bottom pressure recorder measurements at both ends of the loch, and was expected from the daily pumping and release of water from/to Loch Ness for generating hydroelectric power. We also found agreement between glider pitch and PPP GPS heights at periods of less than 4 s, typical of surface gravity waves, suggesting the GPS Wave Glider is also able to capture high-frequency surface signals. The PPP GPS mode 1-s glider ellipsoidal heights had a standard deviation of 0.023 m when compared with heights from relative GPS, with respect to GPS reference stations at both ends of the loch and no more than around 20 km distant at any time. This

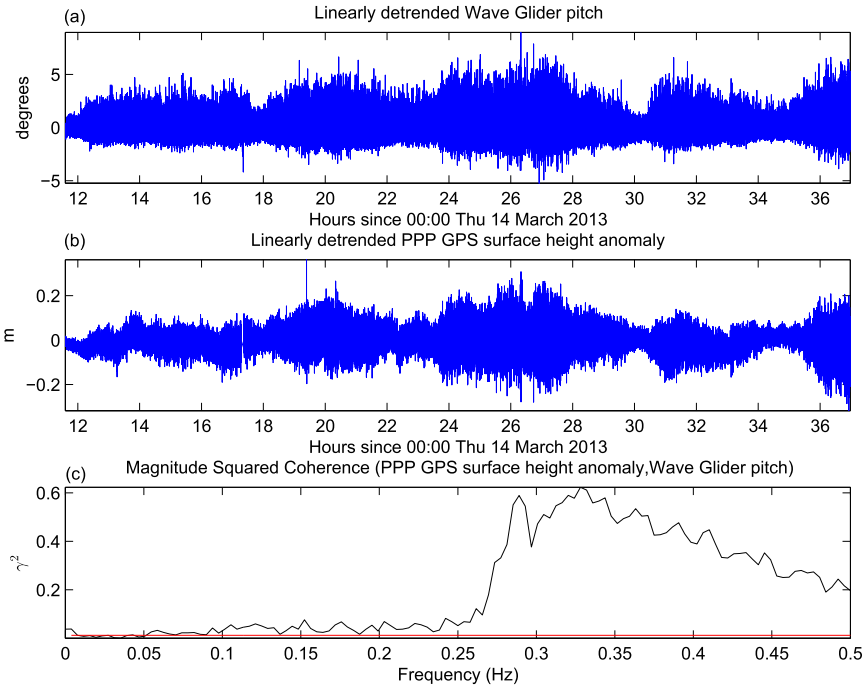

FIG. 5. (a) Linearly detrended, 1-s Wave Glider pitch (°). The trend amounts to an insignificant $-0.005°\,h^{-1}$. (b) PPP GPS 1-s surface height anomalies, having subtracted the EGM2008 geoid height and FAS tide gauge elevations from the GPS ellipsoidal heights. The mean value of the resulting time series has been removed, together with a residual linear trend of $\sim 9 \times 10^{-4}\,m\,h^{-1}$. (c) Magnitude-squared coherence between Wave Glider pitch and PPP GPS surface height anomalies (black curve) calculated following Welch's averaged modified periodogram method. The red curve represents the 99% confidence coherence threshold for independent pitch and height time series [according to Eq. (7) of Miles 2011].

demonstrates the potential of the GPS Wave Glider for centimeter-level surface height measurement globally for lake modeling and altimetry quality control (e.g., Birkett and Beckley 2010) and in the open ocean during benign sea states, as the PPP method does not require nearby reference station data, only accurate satellite orbits and clocks computed from a global network of tracking stations.

It is pertinent to reiterate here that our experiment took place in mild weather conditions, accompanied by calm to slight sea states, ideal therefore to test the optimum performance of the system in an environment with low dynamical noise. Surface conditions in the open ocean tend to be less benign, although sea states between 0 and 3, comparable to those encountered by us in Loch Ness, are not rare. For example, as stated in section 1, in the western North Sea they occur more than 40% of the time between May and August, and even in winter they have a time frequency of about 10% (Fugro GEOS 2001). The Global Atlas of Ocean Waves: Based on VOS Observations (Gulev et al. 2003a,b) shows that, at any given time, sea states between 0 and 3 cover about 5% of the World Ocean's area, mostly in equatorial areas but extending well into the mid- and high-latitude Pacific and Atlantic Oceans during the Northern Hemisphere summer. The response of the Wave Glider to more vigorous wave fields (e.g., Kraus 2012) and the ways in which high-frequency platform motions, white capping, and breaking waves affect the precision of the GPS time series require detailed investigation and the conduction of fieldwork in harsher conditions than experienced in Loch Ness. However, given that we use high-rate GPS data (e.g., here 1 Hz), and providing GPS signal tracking is maintained, we would still anticipate being able to measure tidal and geoid/MDT signals in harsher conditions, as the lower-frequency parts of the GPS time series are not likely to be substantially degraded by wind and swell wave signals with periods of at most a few seconds.

These results testify to the suitability and promise of the novel GPS Wave Glider technology to provide centimeter-precision measurements of sea surface height, fully autonomously and in regions not readily accessible to the deployment of conventional tide gauges, GPS buoys, or bottom pressure recorders.

Acknowledgments. This work has been funded by the Natural Environment Research Council (NERC) under Grants NE/K005421/1 and NE/K005944/1. Philip Woodworth (NOC) has kindly provided practical and scientific advice throughout the duration of this project. His support is greatly appreciated. We are grateful to Julian Dale (Marine Revolution), who led the deployment and recovery of equipment in Loch Ness. Thanks also to Richard Baggaley and Andy Maginnis (Marine Instrumentation Ltd.) for their support in organizing the fieldwork. The help and technical advice of François Leroy, John Applegren, and Mike Cookson (Liquid Robotics, Inc.) are greatly appreciated, as are the helpful discussions with Will Featherstone (Curtin University). Thanks to Louise Robertson (Foyers Primary School) and Jenny MacKenzie (Old Pier House B&B) for accepting our requests for deploying our equipment in their premises. Thanks also to Trimble for lending a GPS unit; to NERC BIGF for the 1-s GPS data; to the Massachusetts Institute of Technology (MIT) for the GAMIT Track software; to NASA JPL for the GIPSY software and satellite orbits and clocks; to Becky Thomson (SEPA) for the tide gauge data at Fort Augustus; and to the Met Office, from whose MIDAS archive we extracted wind data for the Loch Ness area. The maps and graphs were drawn with Generic Mapping Tools software (Wessel and Smith 1998).

REFERENCES

Birkett, C. M., and B. Beckley, 2010: Investigating the performance of the Jason-2/OSTM radar altimeter over lakes and reservoirs. *Mar. Geod.*, **33**, 204–238, doi:10.1080/01490419.2010.488983.

Boehm, J., A. Niell, P. Tregoning, and H. Schuh, 2006a: Global Mapping Function (GMF): A new empirical mapping function based on numerical weather model data. *Geophys. Res. Lett.*, **33**, L07304, doi:10.1029/2005GL025546.

——, B. Werl, and H. Schuh, 2006b: Troposphere mapping functions for GPS and very long baseline interferometry from European Centre for Medium-Range Weather Forecasts operational analysis data. *J. Geophys. Res.*, **111**, B02406, doi:10.1029/2005JB003629.

Bonnefond, P., and Coauthors, 2003: Leveling the sea surface using a GPS-catamaran. *Mar. Geod.*, **26**, 319–334, doi:10.1080/714044524.

Cardellach, E., D. Behrend, G. Ruffini, and A. Rius, 2000: The use of GPS buoys in the determination of oceanic variables. *Earth Planets Space*, **52**, 1113–1116, doi:10.1186/BF03352340.

Chen, J., H. Li, B. Wu, Y. Zhang, J. Wang, and C. Hu, 2013: Performance of real-time precise point positioning. *Mar. Geod.*, **36**, 98–108, doi:10.1080/01490419.2012.699503.

Daniel, T., J. Manley, and N. Trenaman, 2011: The Wave Glider: Enabling a new approach to persistent ocean observation and research. *Ocean Dyn.*, **61**, 1509–1520, doi:10.1007/s10236-011-0408-5.

Foster, J. H., G. S. Carter, and M. A. Merrifield, 2009: Ship-based measurements of sea surface topography. *Geophys. Res. Lett.*, **36**, L11605, doi:10.1029/2009GL038324.

——, B. A. Brooks, D. Wang, G. S. Carter, and M. A. Merrifield, 2012: Improving tsunami warning using commercial ships. *Geophys. Res. Lett.*, **39**, L09603, doi:10.1029/2012GL051367.

Fugro GEOS, 2001: Wind and wave frequency distributions for sites around the British Isles. Health and Safety Executive Offshore Technology Rep. 2001/030, 272 pp.

Gommenginger, C., P. Thibaut, L. Fenoglio-Marc, G. Quartly, X. Deng, J. Gómez-Enri, P. Challenor, and Y. Gao, 2011: Retracking altimeter waveforms near the coasts. *Coastal Altimetry*, S. Vignudelli et al., Eds., Springer-Verlag, 61–101, doi:10.1007/978-3-642-12796-0.

Gulev, S. K., V. Grigorieva, and A. Sterl, 2003a: Global atlas of ocean waves: Based on VOS observations. [Available online at http://www.sail.msk.ru/atlas/.]

——, ——, ——, and D. Woolf, 2003b: Assessment for the reliability of wave observations from voluntary observing ships: Insights from the validation of a global wind wave climatology based on voluntary observing ship data. *J. Geophys. Res.*, **108**, 3236, doi:10.1029/2002JC001437.

Huthnance, J. M., 2004: Ocean-to-shelf signal transmission: A parameter study. *J. Geophys. Res.*, **109**, C12029, doi:10.1029/2004JC002358.

Jevrejeva, S., A. Grinsted, J. C. Moore, and S. Holgate, 2006: Nonlinear trends and multiyear cycles in sea level records. *J. Geophys. Res.*, **111**, C09012, doi:10.1029/2005JC003229.

Kraus, N. D., 2012: Wave Glider dynamic modeling, parameter identification and simulation. Ph.D. thesis, University of Hawai'i at Mānoa, 135 pp.

Kuo, C.-Y., and Coauthors, 2012: High-frequency sea level variations observed by GPS buoys using precise point positioning technique. *Terr. Atmos. Oceanic Sci.*, **23**, 209–218, doi:10.3319/TAO.2011.10.05.01(Oc).

Miles, J. H., 2011: Estimation of signal coherence threshold and concealed spectral lines applied to detection of turbofan engine combustion noise. *J. Acoust. Soc. Amer.*, **129**, 3068–3081, doi:10.1121/1.3546097.

Moore, T., K. Zhang, G. Close, and R. Moore, 2000: Real-time river level monitoring using GPS heighting. *GPS Solutions*, **4**, 63–67, doi:10.1007/PL00012843.

Palanisamy, H., A. Cazenave, O. Henry, P. Prandi, and B. Meyssignac, 2015: Sea-level variations measured by the new altimetry mission SARAL/AltiKa and its validation based on spatial patterns and temporal curves using Jason-2, tide gauge data and an overview of the annual sea level budget. *Mar. Geod.*, **38**, 339–353, doi:10.1080/01490419.2014.1000469.

Pavlis, N. K., S. A. Holmes, S. C. Kenyon, and J. K. Factor, 2012: The development and evaluation of the Earth Gravitational Model 2008 (EGM2008). *J. Geophys. Res.*, **117**, B04406, doi:10.1029/2011JB008916.

——, ——, ——, and ——, 2013: Correction to "The development and evaluation of the Earth Gravitational Model 2008 (EGM2008)." *J. Geophys. Res. Solid Earth*, **118**, 2633, doi:10.1002/jgrb.50167.

Petit, G., and B. Luzum, Eds., 2010: IERS conventions (2010). IERS Tech. Note 36, 179 pp.

Prandi, P., A. Cazenave, and M. Becker, 2009: Is coastal mean sea level rising faster than the global mean? A comparison between tide gauges and satellite altimetry over 1993–2007. *Geophys. Res. Lett.*, **36**, L05602, doi:10.1029/2008GL036564.

Pugh, D. T., P. L. Woodworth, and M. S. Bos, 2011: Lunar tides in Loch Ness, Scotland. *J. Geophys. Res.*, **116**, C11040, doi:10.1029/2011JC007411.

Rocken, C., J. Johnson, T. van Hove, and T. Iwabucki, 2005: Atmospheric water vapour and geoid measurements in the open ocean with GPS. *Geophys. Res. Lett.*, **32**, L12813, doi:10.1029/2005GL022573.

Watson, C., R. Coleman, N. White, J. Church, and R. Govind, 2003: Absolute calibration of TOPEX/Poseidon and Jason-1 using GPS buoys in Bass Strait, Australia. *Mar. Geod.*, **26**, 285–304, doi:10.1080/714044522.

——, ——, and R. Handsworth, 2008: Coastal tide gauge calibration: A case study at Macquarie Island using GPS buoy techniques. *J. Coastal Res.*, **24**, 1071–1079, doi:10.2112/07-0844.1.

Welch, P. D., 1967: The use of fast Fourier transform for the estimation of power spectra: A method based on time averaging over short, modified periodograms. *IEEE Trans. Audio Electroacoust.*, **15**, 70–73, doi:10.1109/TAU.1967.1161901.

Wessel, P., and W. H. F. Smith, 1998: New, improved version of generic mapping tools released. *Eos, Trans. Amer. Geophys. Union*, **79**, 579, doi:10.1029/98EO00426.

Willcox, S., J. Manley, and S. Wiggins, 2009: The Wave Glider, an energy-harvesting autonomous surface vessel. *Sea Technol.*, **50**, 29–32.